DEVELOPMENT OF AN X-BAND PWT PHOTOINJECTOR*

D. Newsham, Y. Luo, J. Zeng, D. Yu, DULY Research Inc., Rancho Palos Verdes, CA 90275
J. Rosenzweig, University of California, Los Angeles, CA 90024

Abstract

Development of an X-band Plane-Wave-Transformer (PWT), integrated photoinjector continues. Modifications of the end-cell design in this two-section device allow for simultaneous frequency and phase tuning of the accelerating field, thus preventing deceleration at the drift region that separates the two sections. The Los Alamos version of PARMELA is used to determine the expected performance parameters from the final design.

1 INTRODUCTION

We report progress on the development of the X-band (8547 MHz) PWT [1][2] integrated photoelectron linear accelerator. The DULY X-band PWT photoinjector (XPWT), shown in Figure 1, consists of two standing wave structures separated by a short drift section. This two-section design was chosen to ease the requirement for reflected power isolation [3]. After balancing the simulation performance with the mechanical and manufacturing restrictions, a final design has been frozen and construction has begun.

X-Band PWT Photoinjector
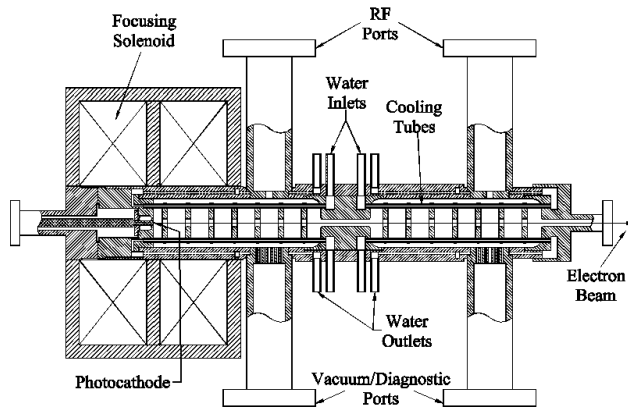
Figure 1: Schematic of the X-Band PWT Photoinjector.

2 DESIGN FEATURES

2.1 All Copper

The primary modification to the design of XPWT was to use all copper parts in the cavity construction. Results from a GdfidL [4] simulation of the earlier S-Band PWT [3] show that significant reduction of the Q-factor of the cavity will occur if the resistivity of the tank wall and cooling tubes is increased. The original design anticipated that the cavity walls and the end plates in each cavity section would be constructed of copper plated stainless steel. To avoid any potential contamination or degradation due to these plated surfaces, both accelerator sections were redesigned to create an all copper cavity, except for the braze joints which most likely play a significant role in the reduction of the cavity Q-factor.

2.2 Focusing Magnet

One of the exciting aspects of the proposed design of the XPWT was the use of permanent magnet material for the focusing field. This resulted in a magnet design that was significantly smaller than would be required using an electromagnet. In addition, the problem of magnet size only becomes worse as the operating frequency is increased, because the strength of the field required for focusing and emittance compensation scales with frequency [5].

Unfortunately, a permanent magnet precludes the ability to alter the strength of the magnetic field by more than a few percent (using trim coils in a hybrid magnet [3]). As a prototype device designed for research applications, the ability to vary the strength of the magnetic field in the laboratory is required to achieve optimal performance, and to provide the versatility needed to make the photoinjector useful in a wide range of applications. In applications where the required magnetic field is fixed and knowable, permanent magnets remain a viable and preferable choice because of the smaller size, stability, and efficiency.

2.3 End Cell Design

To improve the efficiency of acceleration, the design of the 3 transition half-cells (entrance and exit of the drift tube, and the final exit tube) were carefully investigated. Ideally, these cells would be tuned so that at the correct resonant frequency, the position of the electric field maximum would be in phase with the electron beam. By doing so, these cells would become actively accelerating. For a closed half-cell, the solid wall results in an electric field maximum, but when an aperture is opened in the center of the cell wall, the electric field is "pulled" into the aperture and the electric field maximum shifts away from the wall, primarily resulting in energy spread. If the wall shape and position are properly chosen, the apertured half-cell can give the proper phase and frequency of the electric field as shown in the 2D SUPERFISH simulation results in Figures 2 and 3. For the final mechanical design, the features of the cell were simulated in 3D using GdfidL. For design purposes, the 3D dimensional simulation was necessary to properly model the effect of the cooling tubes.
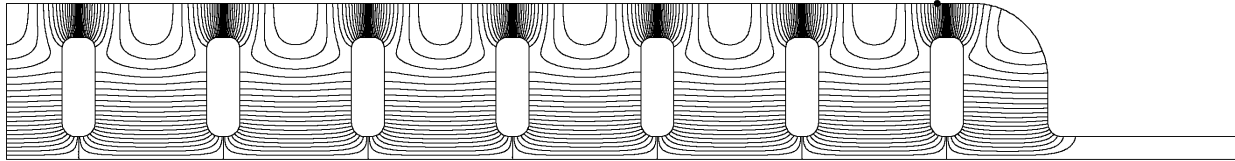
Figure 2: SUPERFISH model of the 6+2/2-cell "first" linac section for the X-band PWT.

Z (units of ½-cell)
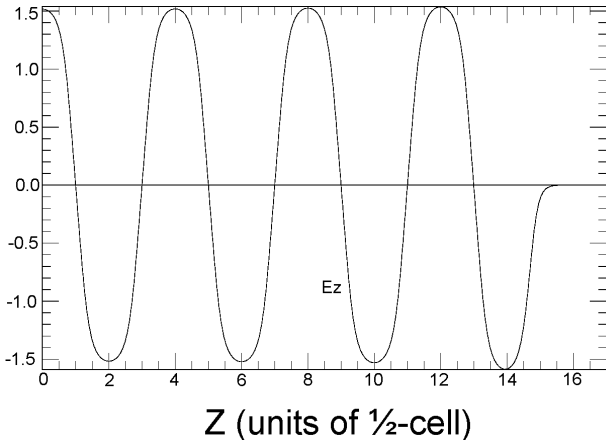
Figure 3: Axial electric field plot for the X-band PWT.

2.4 Cooling

The preliminary design for the disk and tank cooling used 4 separate water circuits. Each section would be cooled independently and the tank wall would be separated from the disk structure. Previously, the tank wall was cooled with a flow channel created between the outer wall of the tank and a brazed cooling jacket. Conversion of the tank material from stainless steel to copper provides better heat transfer, and consequently the same overall cooling can be provided more efficiently.

The first change in the cooling was to use round cooling channels drilled directly into the tank wall. This design eliminates the need for a full water jacket – only the circumferential mixing and inlet/outlet reservoirs require jacketing. This change in tank cooling allowed the disk cooling flow to be placed in series with the tank cooling, as opposed to the original design which used separate circuits. The end result is a halving of the number of water inlet/outlets and a dramatic simplification of the photocathode insertion and end plate design.

2.5 Cathode Attachment

Modification of the water flow design provided room to increase the radial size of the cathode insertion area. In the current design, the photocathode is demountable for replacement. Future uses may require more frequent replacement of the photocathode under vacuum due to heavy use. The increase in the space available for the cathode insertion results in a simplification of the design and will result in easier conversion to a "load-lock" [6] cathode design.

2.6 Combined Vacuum and Diagnostic Ports

The original design of the XPWT had rf feed in both sections, but only the first section had a vacuum port and the second section had a diagnostic port. This placement of the ports was natural since good vacuum is generally most critical at the photocathode; diagnostic knowledge of the electron beam is most useful near the injector exit. It was anticipated that the good vacuum characteristics of the PWT design would provide sufficient pumping on the second section from the first section via the drift tube and from the later vacuum chamber via the exit tube. The similarity of the design of these two ports led to a natural combination. A simple T-fitting will provide straight access for the diagnostic probe, and the vacuum pump can be attached at a right angle. This modification will provide increased vacuum pumping and the ability to diagnose the electron beam in each of the two sections.

3 PARMELA SIMULATION

Three variations of the basic design were studied: 5+2/2-cell, 6+2/2-cell, and 7+2/2-cell. In addition, PARMELA simulations were performed under various assumptions of the degradation of the cavity Q-factor. Each section variant was simulated assuming Q values of 100%, 75%, and 50% of the value calculated using GdfidL and a klystron power of 19 MW divided equally between the two sections. The peak electric field for the simulations is shown in Table 1.

Table 1: Peak Electric Field used in Simulation (MV/m)

	5+2/2	6+2/2	7+2/2
100% Q	160.4	146.3	139
75% Q	139	126.5	120.3
50% Q	113.5	103.3	98.2

3.1 Section Variations

Figures 4, 5, and 6 show simulation results for all 3 structures under the assumption of no cavity degradation. Table 2 gives a summary of the PARMELA results.
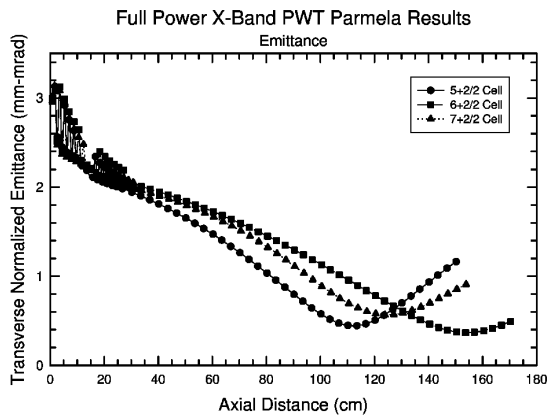
Figure 4: Normalized emittance for 3 design variations.
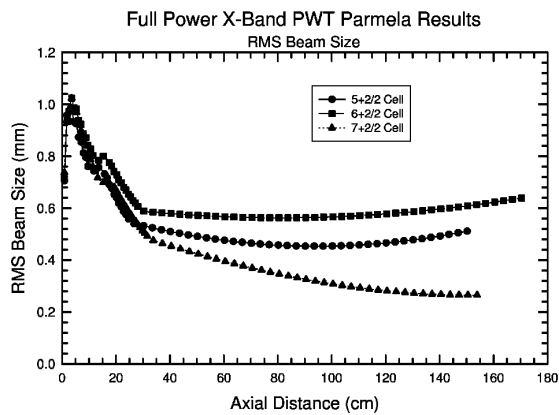
Figure 5: Beam size for 3 design variation
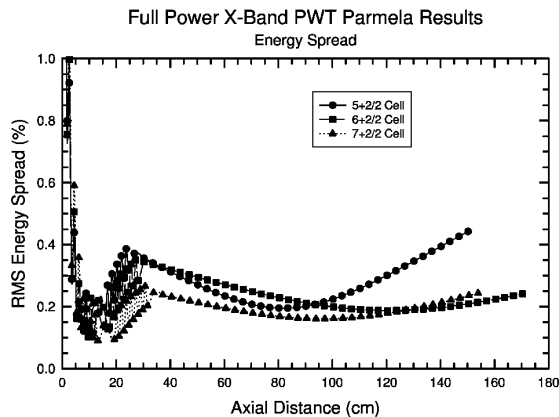
Figure 6: Energy spread for 3 design variation.

3.2 Q Variations

Results from measurements of the S-band PWT installed at UCLA [3] show a value of Q that is approximately 50% of the value calculated using GdfidL. This is the main reason why the cavity was redesigned to be made entirely of copper (Section 2.1). Based on the results of the simulations, the 6+2/2 cell design was

Table 2: Summary of Simulation Results for 3 Structures.

	5+2/2	6+2/2	7+2/2
Frequency (MHz)		8547	
Charge (nC)		0.5	
Transverse Emit (mm-mrad)	.45	.38	.57
Beam Energy (MeV)	18.4	20.7	21.8
Bunch Length (psec)	0.44	0.50	0.55
Beam Radius (mm)	0.5	0.6	0.3
Brightness 10^{15} A/(m-rad)^2	3.2	4.0	1.6

chosen for construction. This design balanced the space requirements needed for the magnetic field coils and access ports with the electric field requirements to capture and efficiently accelerate the electron beam for all 3 Q degradation levels. Figure 7 shows the emittance for the 6+2/2 cell structure for different values of the cavity degradation.
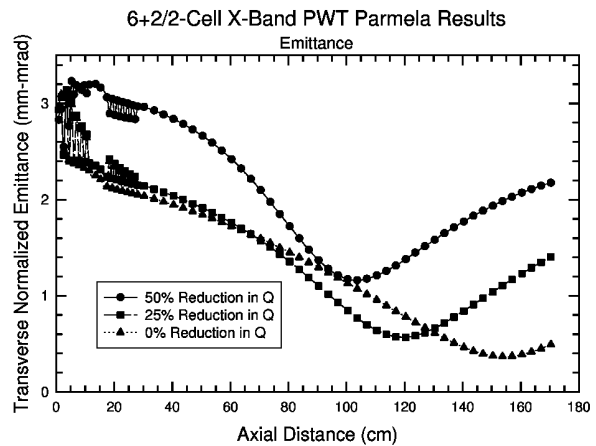
Figure 7: Emittance results from PARMELA model of the 6+2/2 cell XPWT using various values of the degraded Q.

4 REFERENCES

[1] D. Yu *et al.*, Proc. of Part Accel. Conf., New York, NY, March 1999, p.2203.

[2] V.B. Andreev, Soviet Physics – Technical Physics, 13, 1070 (1969); D.A. Swenson, Euro. Part. Accel. Conf., Rome, Italy, ed. S. Atzzart, 2 (1988).

[3] D. Yu, D. Newsham, J. Zeng, and J. Rosenzweig, "S-Band and X-Band Integrated PWT Photoelectron Linacs," AAC2000, Proceedings of the 9th Workshop on Advanced Accelerator Concepts, Santa Fe, New Mexico, June 10-16, 2000.

[4] W. Bruns, Proc. Part. Accel. Conf., Vancouver, B.C., Canada, May 1997, p. 2651.

[5] J. Rosenzewig, *et al.*, Proc. Adv. Accel. Concepts, p. 724, AIP 335, 1995.

[6] R. Bossart, *et al.*, Nucl. Instrum. Meth. A375:ABS7-ABS8, 1996, CERN-PS-95-33-RF, Sep. 1995, CLIC Note 297 or R.E. Kirby *et al.*, Proc. of Part Accel. Conf., Washington D.C., May 1993, p.3030, SLAC-PUB-6006.